Chiral supramolecular nanotubes of single-chain magnets

Chiral supramolecular nanotubes of single-chain magnets

Felix Houard,[a] Quentin Evrard,[a] Guillaume Calvez,[a] Yan Suffren,[a] Carole Daiguebonne,[a] Olivier Guillou,[a] Frédéric Gendron,[a] Boris Le Guennic,[a] Thierry Guizouarn,[a] Vincent Dorcet,[a] Matteo Mannini,[b] and Kevin Bernot*[a]

Abstract: We report a Single-Chain Magnet (SCM) made of a Terbium(III) building block and a nitronyl-nitroxide radical (NIT) functionalized with an aliphatic chain. This substitution is targeted to induce a long range distortion of the polymeric chain and accordingly it gives rise to chains that are curled with almost 20 nm helical pitch. They self-organize as a chiral tubular superstructure made of 11 chains wound around each other. The supramolecular tubes have a 4.5 nm internal diameter. Overall, this forms a porous chiral network with almost 44% porosity. Ab-initio calculations highlight that each Tb^{III} ion possesses high magnetic anisotropy. Indeed, notwithstanding the supramolecular arrangement each chain behaves as a SCM. Magnetic relaxation with both finite and infinite-size regimes is observed and confirms the validity of the Ising approximation. This is associated with quite strong coercive field and magnetic remanence (H_c = 2400 Oe M_R = 2.09 μ_B at 0.5 K) for this class of compounds.

Single-chain magnets (SCM) are one-dimensional analogues of single-molecules magnets that are objects able to act as magnets at the molecular level. SCMs have attracted attention because of the strong robustness of their molecular magnetic relaxation towards tunnelling effects.[1] These one-dimensional structures exhibit magnetic bistability at the molecular level thanks to the strong anisotropy of their spin carriers, their strong intramolecular magnetic exchange and good magnetic insulation.[2] Among them, chains made of nitronyl-nitroxide (NIT) organic radicals[3] and 3*d* [4] or 4*f* [5] ions show significant SCM behaviour.

Here, we have synthesized a novel NIT radical derivative namely NIT-Ph-O-Hexyl (2-(4'-hexoxyphenyl)-4,4,5,5-tetramethylimidazolin-1-oxyl-3-oxide). Its aromatic group ensures the chain robustness (intra-chain π-stacking interactions) and is connected in *para* to an aliphatic tail (Figure S1, Table S1). This latter possesses large degrees of freedom targeted to give rise to large crystallographic asymmetric unit because of the huge variety of structural conformations that it could accommodate. The stoichiometric reaction of NIT-O-hexyl with the $[Tb(hfac)_3{\cdot}2H_2O]$ building block ($hfac^-$ = hexafluotoacetylacetonate) affords thin cyan needles of formula $[Tb(hfac)_3NIT\text{-}O\text{-}Hexyl]_n$ latter named **TbNIT-Ph-O-Hexyl** (Experimental Section, Figures S2-S4). It crystallizes in a hexagonal system, chiral $P6_122$ space group (N°178). The cell volume is rather large, V = 54727 Å^3 (Tables S2-S3). The asymmetric unit is made of two and a half radicals and two and a half terbium atoms (Tb1, Tb2, Tb3) that alternate (Figure 1). One terbium atom (Tb1) and one radical (central atom C80) lay on a 2-fold symmetry axis that lies along *a* and *a+b* respectively. This generates a chain that grows along the *c* direction. Continuous Shape Measurements (CShM)[6] show that the Tb(III) coordination polyhedron are slightly distorted triangular dodecahedron ($Tb1_{CShM}$ = 0.51; $Tb2_{CShM}$ = 0.45) or square antiprism ($Tb3_{CShM}$ = 0.80) (Table S4). Shortest Tb-Tb distance is 8.39 Å.

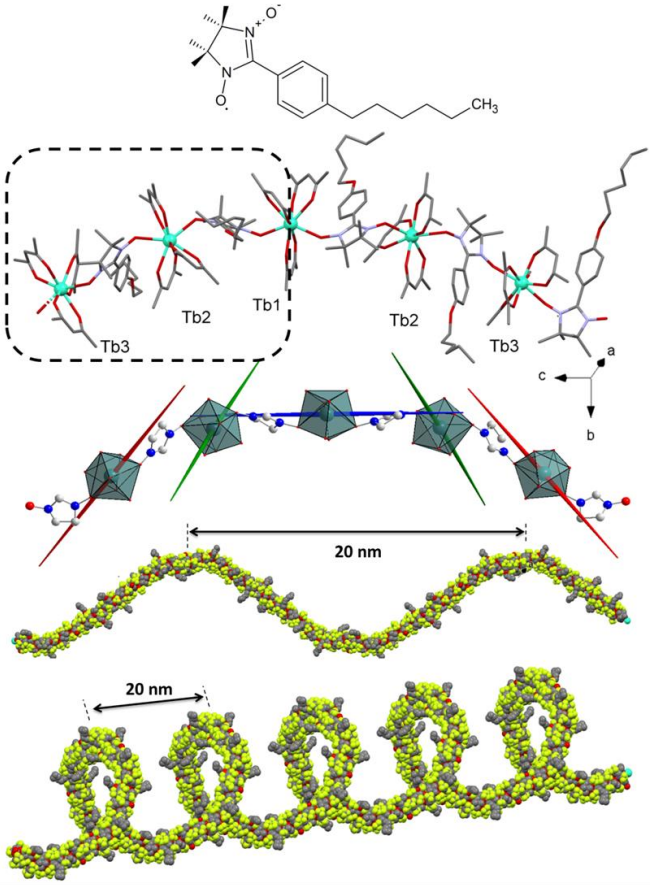

Figure 1. (top) Scheme of the **NIT-Ph-O-Hexyl** radical (middle) Representation of the **TbNIT-Ph-O-Hexyl** chain with the asymmetric unit as dotted square, a view with the NIT skeleton and Tb coordination polyhedra represented together with easy magnetic axes computed from ab-initio calculations (Tb1 blue, Tb2 green and Tb3 red) and (bottom) Representation of the chain with atoms represented with their van der Waals radii (along *b* axis and slightly away from it), 5 curls are drawn representing 60 units cells

The NIT-4*f* chains[3] can be described by the Cx-Ln-Cx angle where Cx is the central C atom of the tetramethylimidazoline

[a] F. Houard, Dr Q. Evrard, Dr. G. Calvez, Dr. Y. Suffren, Dr C. Daiguebonne, Pr. O. Guillou, Dr. F. Gendron, Dr. B. Le Guennic, Dr. V. Dorcet, T. Guizouarn, and Dr. K. Bernot*
Univ Rennes, INSA Rennes, CNRS, ISCR (Institut des Sciences Chimiques de Rennes), UMR 6226, F-35000 Rennes, France.
E-mail: kevin.bernot @insa-rennes.fr

[b] Prof. M. Mannini,
LAboratory for Molecular Magnetism (LA.M.M.)
Dipartimento di Chimica "Ugo Schiff"
Università degli Studi di Firenze,INSTM,UdR Firenze
Via della Lastruccia n. 3
Sesto Fiorentino (FI) 50019 ITALY

Supporting information for this article is given via a link at the end of the document.

group. Usually, two consecutive angles compensate along the chain direction to give rise to a regular and flat zig-zag chain.[7] In **TbNIT-Ph-O-Hexyl**, the picture is very different. All Cx-Ln-Cx angles add up to form an asymmetric unit bent by 16.4°. This bending, combined with the 2-, 3- and 6-fold symmetry axes, creates a helicoïdal chain along the *c* axis. 12 asymmetric units are necessary to make a full revolution.

The pitch length is almost 20 nm (198 Å) (Figure 1). As anticipated this arrangement is due to the flexibility of the hexyl tail of the NIT-O-hexyl radical that accommodates very different structural conformations along the asymmetric unit, a feature not possible with more rigid NIT radicals.[8] The crystal packing of these chains is even more peculiar since the long helical pitch creates room for 10 other chains. Overall, 11 chains are wound around each other and give rise to a self-organized chiral tubular superstructure along the *c* axis (Figure 2). These neighbouring chains are generated by the symmetry axes of the $P6_122$ space group (this space group has 12 symmetry operations but one of the chains lies in special position). The resulting structure is a nanotube with an external diameter of 6.8 nm and an inner bore of 4.5 nm filled by disordered heptane molecules (Figure 3). There is one nanotube per unit cell and so all nanotubes are crystallographically similar (Figure 3). The shortest intermolecular Tb-Tb distance is then 11.3 Å while it is 8.3 Å within a chain.

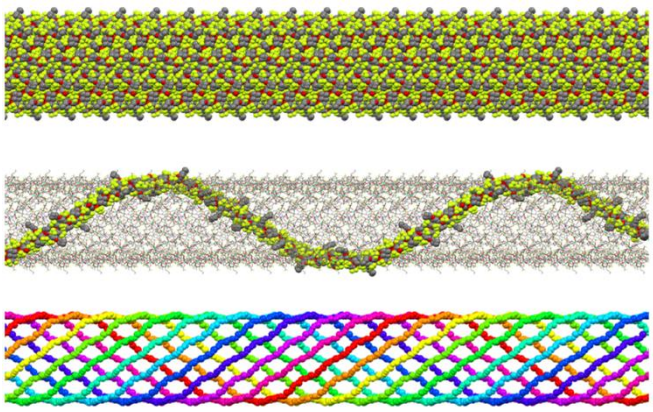

Figure 2. Representation of the supramolecular nanotube formed by **TbNIT-Ph-O-Hexyl** chains along the *b* crystallographic axis (terminal alkyl chains, hydrogens and solvent molecules omitted): (top) Atoms represented with their van der Walls radii; (middle) One chain with van der Walls radii; (bottom) The eleven curled chains that forms one nanotube, with only the magnetic backbone represented (C-N-O-Tb-N-O-C-N atoms).

On the tested crystal, the eleven chains are curled clockwise. It could be stressed that this chirality, as in similar chains[9] comes from the spontaneous resolution in the $P6_122$ chiral space group. In the absence of chiral building blocks the opposite chirality ($P6_522$) is equally probable but it has not been searched given the complexity of crystal structure data collection and analysis.

The evident affinity between the reaction solvent (heptane) and the aliphatic tail of the radical plays a key role in the thermodynamic stabilization of these nanotubes. One can make the hypothesis that the helical arrangement is induced by the heptane molecules trapped via aliphatic π-interactions.[10]

The calculated porosity is 25495 $Å^3$ (44% of cell volume for a 1.2 Å kinetic radius, Figure S5). When taken out of the mother solution the crystals quickly lose their crystallinity and X-ray diffracting power but not their crystal shape. This is visible on SEM images where crystal bending is observed under vacuum (Figures 5, S6). Similarly, on one minute air-dried samples no trace of heptane can be found either by thermogravimetric analyses (TGA) (Figure S7) or coupled TGA-FTIR (no IR signature of heptane in the TGA exhaust gases, Figure S8). The compound is stable up to $T_{melting}$ = 120°C, close to the value observed on other Ln-NIT chains not structured as nanotubes.[5b]

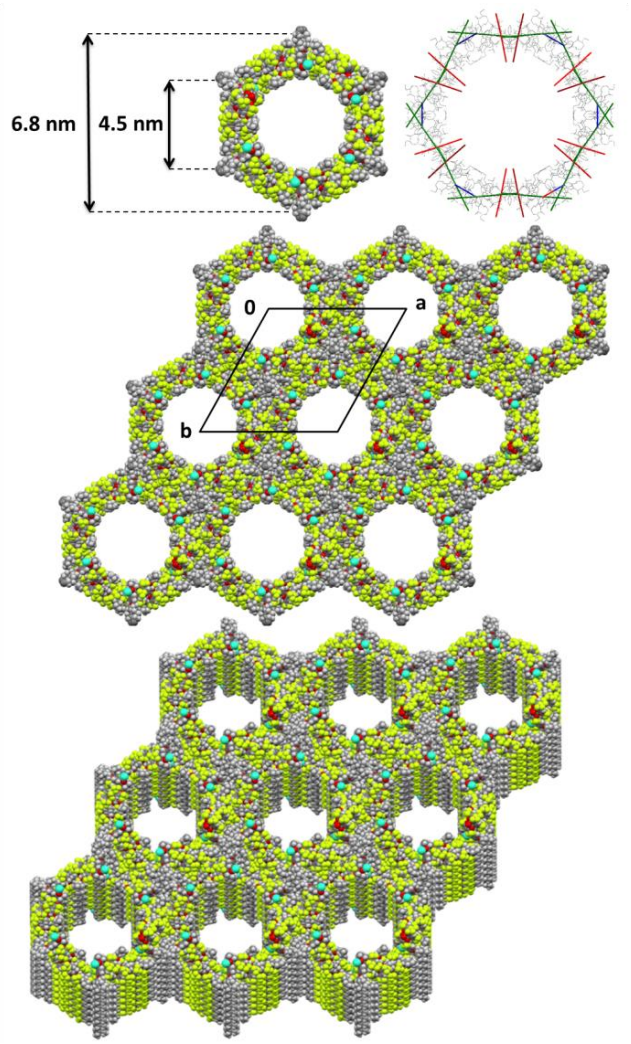

Figure 3. (top) Representation of a nanotube of **TbNIT-Ph-O-Hexyl** with calculated magnetic axes; (middle) Representation of the crystal packing along the *c* axis; (bottom) Perspective view of the crystal packing highlighting the supramolecular nanotubes (solvent molecules omitted).

To further confirm that the chain structure is conserved upon crystallinity loss, solid-state luminescence measurements with varying temperatures have been performed. We have targeted

the strong luminescence properties of the chain's building blocks, $[Tb(hfac)_3 \cdot 2H_2O]$ (very intense line-shaped green emission[11]) and NIT radicals (broad-shaped red emission that is blue-shifted upon $Tb(hfac)_3$ coordination[12] that also quenches the Tb^{III} emission). As expected, **TbNIT-Ph-O-Hexyl** shows neither any trace of Tb^{III} nor uncoordinated NIT radical emission (Figures 4 and S9-S15) but a blue-shifted radical luminescence. This makes the air-dried sample suitable for magnetic analyses.

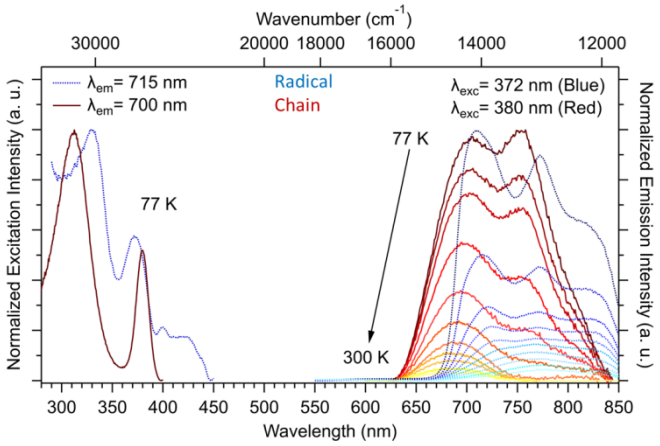

Figure 4. Solid-state excitation spectra at 77 K (λ_{em} = 715 or 700 nm), and emission spectra (λ_{ex} = 372 or 380 nm) measured on **NIT-Ph-OHexyl** uncoordinated radical (blue to green dotted curves) and **TbNIT-Ph-OHexyl** (dark red to yellow curves).

Static magnetic measurements (H_{dc} = 1000 Oe) show a $\chi_M T_{(300K)}$ = 12.44 emu.K.mol^{-1} value, close to the expected value for one isolated radical and one Tb^{III} ion ($\chi_M T_{(300K)}$ = 12.195 emu.K.mol^{-1} with S = 1/2; g_J = 3/2, J = 6). As the temperature is lowered, a severe increase of $\chi_M T$ is observed below 50 K up to $\chi_M T$ = 24.2 emu.K.mol^{-1} at 3.5 K as a result of the onset of a spin correlation along the chain. Below 3.5 K, $\chi_M T$ drops because of saturation effects. To tackle this, dc measurements with lowest field (H_{dc} = 100 Oe) and dynamic (ac) magnetic measurements (H_{ac} = 3 Oe) have been performed (Figure 5). The highest value of $\chi_M T$ is $\chi_M T$ = 26.56 emu.K.mol^{-1} at 3.2 K. Specific heat (C_P) studies down to 2 K do not highlight any abrupt anomaly in the C_P and exclude the presence of 3D magnetic ordering (Figure S16).[13]

If well magnetically shielded, NIT-Ln chains can behave as Ising chains and exhibit Single-Chain Magnet (SCM) behaviour.[14] In such chains, magnetic slow relaxation operates via Glauber mechanism,[15] a relaxation pathway more robust than the Orbach one seen on SMMs.[16] Accordingly, Ising one-dimensional systems present an exponential divergence of $\chi_M T$ as the temperature is lowered[15] such as $\chi_M T = C_{eff}\exp(\Delta_\xi/k_B T)$ with C_{eff} the effective Curie constant, k_B the Boltzmann constant and Δ_ξ the correlation energy. This assumption can be made only in absence of dc field. This is the reason why ac measurement (H_{dc} = 3 Oe) at 1Hz have been considered for Δ_ξ extraction (Figure S17). Values are C_{eff} = 11.84 emu.K.mol^{-1} and $\Delta_{\xi\,(dc)}$ = 5.5 ± 0.5 K (R^2 = 0.9998).

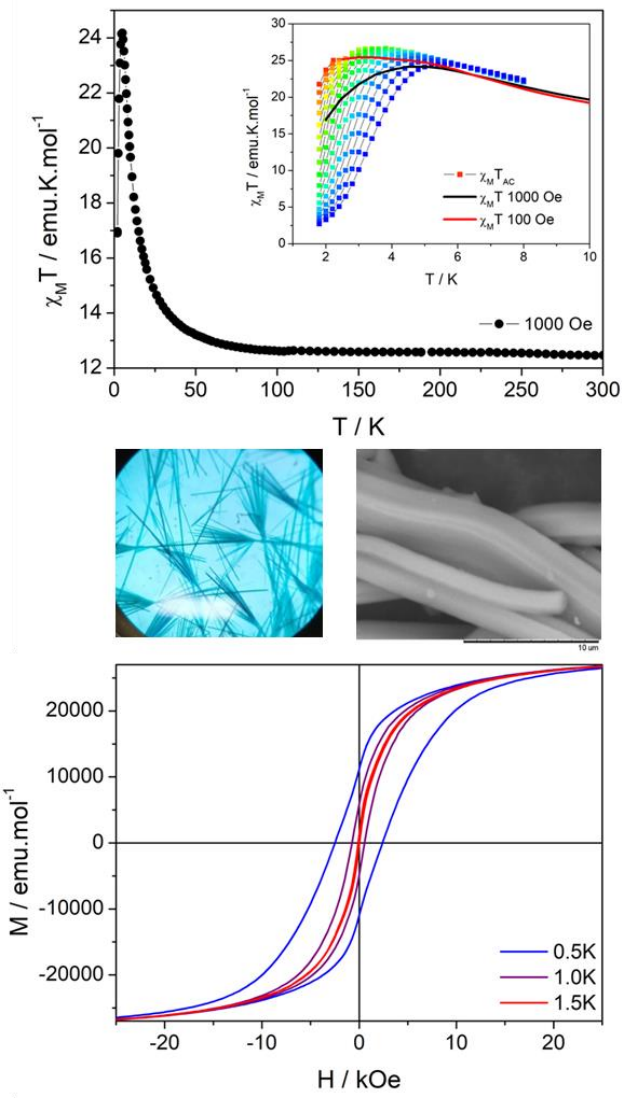

Figure 5. (top) Temperature dependence of $\chi_M T$ with in inset, the low temperature region measured at various dc fields (full line) or reconstructed from ac susceptometry (H_{ac}= 3 Oe) with frequencies from 1500 Hz (blue) to 0.1 Hz (red); (middle) single crystal of **TbNIT-Ph-OHexyl** observed under microscope with X 63 magnification and SEM image of a de-solvated bent crystal; (bottom) Hysteresis curves measured with a magnetic field sweep rate of 15.5 Oe.s^{-1}

We recall that NIT-Ln chains are known to host next-nearest neighbour (NNN) interactions that are expected to be stronger than Ln-NIT ones.[17] This numerous magnetic pathways as well as the three crystallographically different Tb^{III} ions in **TbNIT-Ph-O-Hexyl** hamper a precise quantification of the magnetic couplings in the chain. However, ab-initio calculations indicate that the coordination environment imprints to all terbium ions a strong magnetic anisotropy with their easy magnetic axes that do not lie in any particular direction with respect to the molecule (Figures 1, 3, S18-S21, Tables S5-S6).

Ac susceptibility confirms the SCM behaviour of **TbNIT-Ph-O-Hexyl**. The field dependence of the out-of phase susceptibility (χ_M'') at 2 K is in agreement with what expected for

a SCM with the slowest relaxation observed for H_{dc} = 0 Oe (Figure S22).[18] Temperature dependence of the magnetic relaxation is observed up to 7 K (Figures 6, S23-S25) and relaxation times (τ) are fitted via an Arrhenius law ($\tau = \tau_0 \exp(\Delta_{eff}/k_BT)$) where Δ_{eff} is the effective energy barrier (Table S7). On SCM, different values of Δ_{eff} can be observed depending if infinite- ($\Delta_I = \Delta_A + 2\Delta_\xi$) or finite-size ($\Delta_F = \Delta_A + \Delta_\xi$) regime operates (with Δ_A, the energy barrier due to the Tb^{III} ion).[15] In our case, Δ_I = 29.6 ± 0.5 K (τ_0 = (3.4 ± 0.5) x 10^{-8} s) and Δ_F = 25.5 ± 0.2 K (τ_0 = (2.4 ± 0.3) x 10^{-7} s) with a crossover between the two regimes observed at T* = 2.1 K.

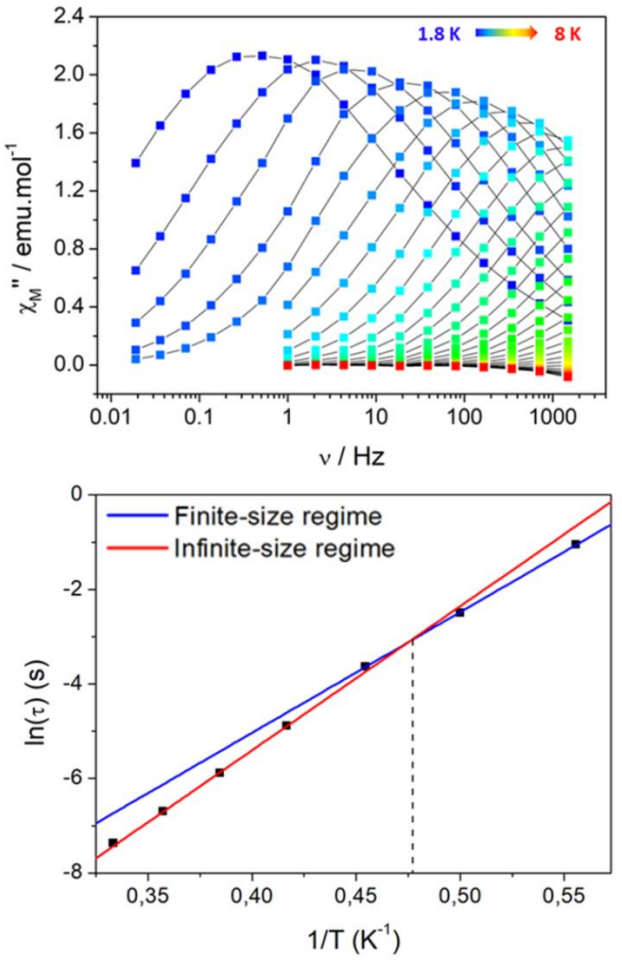

Figure 6. (top) Frequency dependence of the out-of-phase susceptibility measured on **TbNIT-Ph-OHexyl** from 1.8 K (blue) to 8 K (red); (bottom) Arrhenius plot of the relaxation times.

As expected $\Delta_{\xi(ac)} = \Delta_I - \Delta_F$ = 4.1 ± 0.7 K is close to $\Delta_{\xi(dc)}$ = 5.5 ± 0.5 K estimated above. In a SCM, the average number, n, of correlated magnetic units in a chain is given by $n \approx 2\xi \approx \exp(\Delta_\xi/k_BT^*)$. Here, it varies from n = 5 ($\Delta_{\xi\,(ac)}$) to n = 17 ($\Delta_{\xi\,(dc)}$). We recall that this value is purely informative as such treatment is valid for chains made of repeating identical magnetic units. In **TbNIT-Ph-O-Hexyl**, the crystallographic asymmetric unit is made of two and a half Tb^{III} ions and two and a half radicals, which makes the correlation length complex to rationalize.

Last, the distribution (α) of the relaxation times (τ) has been evaluated using Cole-Cole plots (Figure S26, Table S8) and is in line with what is expected for SCMs. It can be noted that at 1.8 K almost all the sample relax slowly ($1-(\chi_s/\chi_T)$ = 93%, where χ_s and χ_T correspond to the adiabatic and the isothermal susceptibility respectively).

Hysteresis measurements have been performed (Figures 5, S27) and in our operating conditions (magnetic field sweep rate of 15.5 $Oe.s^{-1}$) the average τ that gives rise to a hysteresis opening is τ_m = 21.2 s that corresponds to T = 1.39 ± 0.02 K if the finite-size regime is considered. Accordingly, a clear hysteresis opening is observed below 1.5 K, while it is closed at 1.8 K. At 0.5 K, a coercive field of H_c = 2400 Oe and a strong magnetic remanence of M_R = 11700 $emu.mol^{-1}$ (2.09 μ_B) are observed. **TbNIT-Ph-O-Hexyl** thus behaves as a SCM with magnetic hysteresis that has a molecular origin.

In conclusion, functionalization of aromatic NIT radicals by hexyl tail allows obtaining **TbNIT-Ph-O-Hexyl**, a chiral supramolecular arrangement of SCMs in which chains are wound 11 by 11 to form molecular nanotubes. This supramolecular architecture preserve the SCM behaviour of each chain and zero-field opened hysteresis is observed (H_c = 2400 Oe at 0.5 K) with no 3D magnetic ordering. This is in strong contrast with what is commonly seen on mononuclear Ln-SMM where zero-field fast tunnel relaxation is acting. This result recalls other examples of chiral arrangements obtained with NIT radicals.[3-5, 9b, 13a] The stacking interaction between the β-diketonate and the NIT phenyl ring may be the driving force for the creation of these screw chains. **TbNIT-Ph-O-Hexyl** also recalls similar structures with alkyl chains such as homochiral supramolecular subphthalocyanine columns[19], α-cyclodextrin organic nanotubes,[20] or Cu(I) supramolecular helixes.[21]

Additionally, the chiral nature of the nanotubes makes **TbNIT-Ph-O-Hexyl** a good candidate to observe electric field modulation of magnetic exchange[22] or magneto-chiral dichroism[9b] as observed on NIT-based chains with 3d metal ions. Chiral Ln-NIT chain appears very appealing for the coexistence of strong spin-orbit coupling and frustrated magnetic interactions.[23] Last, **TbNIT-Ph-O-Hexyl** shows a huge porosity (44% of cell volume) that opens the way to solvent or gas responsive SCMs with tuneable magnetic properties. These fluorinated and hydrophobic nanopores could also have original transport properties for gas or liquids as observed on nanometric lab-on-a chip devices.[24] [25]

Experimental Section

Experimental details on synthesis, crystal growth, crystallographic studies, FT-IR, SEM, EDS, TGA analyses, magnetic (ac, dc), specific heat, luminescence studies and *ab initio* calculations details are provided as supplementary information. Crystallographic structural files are available from Cambridge Structural Database as CCDC-1958728 (**NIT-Ph-O-Hexyl**) and CCDC-1958799 (**TbNIT-Ph-O-Hexyl).**

Acknowledgements

This work was supported by INSA Rennes, CNRS, MIUR-Italy ("Progetto Dipartimenti di Eccellenza 2018-2022" allocated to Department of Chemistry "Ugo Schiff"). Pr. R. Sessoli is acknowledged for stimulating discussions. Dr T. Roisnel from ISCR CDifX is acknowledged for discussion on crystal structure. Stéphane Freslon is acknowledged for help in STA-FTIR analysis. K.B acknowledges the Institut Universitaire de France (IUF). F.G. and B.L.G. thank the French GENCI/IDRIS-CINES centres for high-performance computing resources. F.G. and B.L.G. acknowledge the Stratégie d'Attractivité Durable (SAD18006 - LnCPLSMM).

Keywords: Single-Chain Magnets • Lanthanides • Radicals • Supramolecular • Nanotubes • Chirality

[1] R. Clérac, H. Miyasaka, M. Yamashita, C. Coulon, *J. Am. Chem. Soc.* **2002**, *124*, 12837-12844.

[2] R. Clérac, R. E. P. Winpenny, in *50 Years of Structure and Bonding – The Anniversary Volume* (Ed.: D. M. P. Mingos), Springer International Publishing, Cham, **2016**, pp. 35-48.

[3] X. Meng, W. Shi, P. Cheng, *Coord. Chem. Rev.* **2019**, *378*, 134-150.

[4] A. Caneschi, D. Gatteschi, N. Lalioti, C. Sangregorio, R. Sessoli, G. Venturi, A. Vindigni, A. Rettori, M. G. Pini, M. A. Novak, *Angew. Chem.-Int. Ed.* **2001**, *40*, 1760-1763.

[5] a) L. Bogani, C. Sangregorio, R. Sessoli, D. Gatteschi, *Angew. Chem.-Int. Edit.* **2005**, *44*, 5817-5821; b) K. Bernot, L. Bogani, A. Caneschi, D. Gatteschi, R. Sessoli, *J. Am. Chem. Soc.* **2006**, *128*, 7947-7956.

[6] S. Alvarez, P. Alemany, D. Casanova, J. Cirera, M. Llunell, D. Avnir, *Coord. Chem. Rev.* **2005**, *249*, 1693-1708.

[7] H. L. Sun, Z. M. Wang, S. Gao, *Coord. Chem. Rev.* **2010**, *254*, 1081-1100.

[8] a) S. Demir, I.-R. Jeon, J. R. Long, T. D. Harris, *Coord. Chem. Rev.* **2015**, *289–290*, 149-176; b) L. Bogani, A. Vindigni, R. Sessoli, D. Gatteschi, *J. Mater. Chem.* **2008**, *18*, 4750-4758.

[9] a) X. Liu, Y. Zhang, W. Shi, P. Cheng, *Inorg. Chem.* **2018**; b) R. Sessoli, M.-E. Boulon, A. Caneschi, M. Mannini, L. Poggini, F. Wilhelm, A. Rogalev, *Nat. Phys.* **2015**, *11*, 69-74.

[10] K. S. Kim, S. Karthikeyan, N. J. Singh, *J. Chem. Theory Comput.* **2011**, *7*, 3471-3477.

[11] K. Binnemans, in *Handbook on the Physics and Chemistry of Rare-Earths, Vol. 35* (Eds.: J. K.A. Gschneider, J. C. G. Bünzli, V. K. Pecharsky), Elsevier B.V., Amsterdam, **2005**.

[12] A. Lannes, M. Intissar, Y. Suffren, C. Reber, D. Luneau, *Inorg. Chem.* **2014**, *53*, 9548-9560.

[13] a) F. Cinti, A. Rettori, M. Barucci, E. Olivieri, L. Risegari, G. Ventura, A. Caneschi, D. Gatteschi, D. Rovai, M. G. Pini, M. Affronte, M. Mariani, A. Lascialfari, *J. Magn. Magn. Mater.* **2007**, *310*, 1460-1461; b) E. Bartolome, J. Bartolome, S. Melnic, D. Prodius, S. Shova, A. Arauzo, J. Luzon, F. Luis, C. Turta, *Dalton Trans.* **2013**, *42*, 10153-10171.

[14] L. Bogani, C. Sangregorio, R. Sessoli, D. Gatteschi, *Angew. Chem.-Int. Ed.* **2005**, *117*, 5967-5971.

[15] R. J. Glauber, *J. Math. Phys.* **1963**, *4*, 294-307.

[16] D. Gatteschi, R. Sessoli, J. Villain, *Molecular Nanomagnets*, Oxford University Press, Oxford, **2006**.

[17] a) M. G. Pini, A. Rettori, *Phys. Rev. B* **1993**, *48*, 3240-3248; b) K. Bernot, J. Luzon, A. Caneschi, D. Gatteschi, R. Sessoli, L. Bogani, A. Vindigni, A. Rettori, M. G. Pini, *Phys. Rev. B* **2009**, *79*, 134419.

[18] C. Coulon, R. Clérac, W. Wernsdorfer, T. Colin, A. Saitoh, N. Motokawa, H. Miyasaka, *Phys. Rev. B* **2007**, *76*, 214422.

[19] J. Guilleme, M. J. Mayoral, J. Calbo, J. Aragó, P. M. Viruela, E. Ortí, T. Torres, D. González-Rodríguez, *Angew. Chem.-Int. Ed.* **2015**, *54*, 2543-2547.

[20] a) T. Shimomura, T. Akai, T. Abe, K. Ito, *J. Chem. Phys.* **2002**, *116*, 1753-1756; b) E. Ikeda, Y. Okumura, T. Shimomura, K. Ito, R. Hayakawa, *J. Chem. Phys.* **2000**, *112*, 4321-4325.

[21] S. Evariste, A. M. Khalil, M. E. Moussa, A. K.-W. Chan, E. Y.-H. Hong, H.-L. Wong, B. Le Guennic, G. Calvez, K. Costuas, V. W.-W. Yam, C. Lescop, *J. Am. Chem. Soc.* **2018**, *140*, 12521-12526.

[22] M. Fittipaldi, A. Cini, G. Annino, A. Vindigni, A. Caneschi, R. Sessoli, *Nat. Mater.* **2019**.

[23] C. Benelli, D. Gatteschi, *Chem. Rev.* **2002**, *102*, 2369-2388.

[24] J. C. T. Eijkel, A. van den Berg, *Chem. Soc. Rev.* **2010**, *39*, 957-973.

[25] L. Bocquet, E. Charlaix, *Chem. Soc. Rev.* **2010**, *39*, 1073-1095.

COMMUNICATION

We report a supramolecular assembly of Single-Chain Magnets (SCM) that self-organize to form chiral supramolecular nanotubes where their magnetic behaviour is preserved.

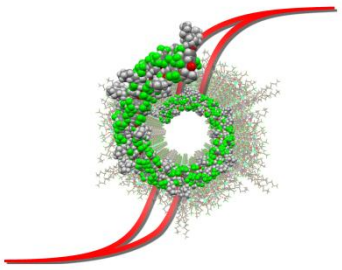

*Felix Houard, Quentin Evrard, Guillaume Calvez, Yan Suffren, Carole Daiguebonne, Olivier Guillou, Frédéric Gendron, Boris Le Guennic, Thierry Guizouarn, Vincent Dorcet, Matteo Mannini and Kevin Bernot**

Page No. – Page No.

Chiral supramolecular nanotubes of single chain magnets